PK-PD modeling of 1-(3-*C*-ethynyl-β-D-*ribo*-pentofuranosyl)cytosine and the enhanced antitumor effect of its phospholipid derivatives in long-circulating liposomes

Akitsugu Takada, Hiroyuki Kamiya*, Satoshi Shuto, Akira Matsuda, Hideyoshi Harashima

Faculty of Pharmaceutical Sciences, Hokkaido University, Kita-12, Nishi-6, Kita-ku, Sapporo 060-0812, Japan

*Corresponding author: Tel: +81-11-706-3733; Fax: +81-11-706-4879; E-mail: hirokam@pharm.hokudai.ac.jp

Abstract

The efficacy of an antitumor nucleoside, 1-(3-*C*-ethynyl-β-D-*ribo*-pentofuranosyl)cytosine (3'-ethynylcytidine, ECyd), was analyzed *in vitro* and *in vivo*. The *in vivo* antitumor effect of ECyd encapsulated into long-circulating liposomes was also examined. Based on pharmacokinetic (PK) and pharmacodynamic (PD) analyses, a model that quantitatively explains the *in vivo* effects of ECyd was proposed, using the concept of minimum effective concentration. The model suggests that ECyd followed a time-dependent mechanism of action *in vivo*, and that availability of ECyd in tumor tissue was highly important. To improve the availability of ECyd, its phospholipid derivatives were synthesized and encapsulated into long-circulating liposomes, which increased the antitumor effect. These results indicate that it is very important to design carriers of antitumor drugs based on PK-PD modeling.

Keywords: 3'-ethynylcytidine; antitumor effect; PK–PD modeling; phospholipid derivatives; liposome; minimum effective concentration

1. Introduction

Antitumor drugs are classified into two groups based on their dose-dependencies [Shimoyama, 1975; Ozawa et al., 1988, 1989]. One is a concentration-dependent drug group, which includes alkylating agents, intercalators and platinum derivatives (type I). Their cytotoxic effect depends on both concentration and exposure time, namely, on the area under the concentration–time curve (AUC). Thus, short exposure to these drugs at high concentration, and long exposure at low concentration, results in similar cytotoxicity. The other group is the exposure time-dependent drug group, which includes antimetabolites and vinca alkaloids (type II). Their cytotoxicity requires a certain exposure period, and short exposure at high concentration does not exert sufficient antitumor activity. Based on studies by Sugiyama's group, cell-cycle independent and dependent antitumor drugs are classified into type I and type II groups, respectively [Ozawa et al., 1988, 1989].

The type I antitumor drugs can be expected to be more effective when a drug delivery system (DDS) increases their AUC. Liposomes are a candidate for useful carriers that encapsulate water-soluble drugs into the aqueous phase and lipid-soluble drugs into the lipid membrane. Polyethylene glycol (PEG)ylation can dramatically prolong liposome circulation time in blood by preventing the absorption of liposomes onto opsonins, serum proteins [Blume and Cevc, 1990; Klibanov et al. 1990; Allen et al., 1991]. Unmodified liposomes disappear from blood circulation due to entrapment by reticuloendothelial system (RES) organs, such as liver and spleen, before they reach tumor tissue. On the other hand, PEGylated long-circulating liposomes can deliver antitumor drugs to tumor tissue by escaping from

recognition by opsonins in blood. The long circulation of the PEG-liposomes is also expected to enhance the antitumor effects of type II drugs, since they can be released for a longer period. Doxorubicin (Dox) and vincristine, AUC-dependent type I and AUC-independent type II antitumor drugs, respectively, have been shown to have enhanced activity after encapsulation into long-circulating liposomes [Papahadjopoulos et al., 1991; Vaage et al., 1993].

An antitumor nucleoside, 1-(3-*C*-ethynyl-β-D-*ribo*-pentofuranosyl)cytosine (3'-ethynylcytidine, ECyd) (Fig. 1), exerts its cytotoxic effect by transcription inhibition and apoptosis induction [Hattori et al., 1996; Tabata et al., 1997; Takatori et al., 1998, 1999]. ECyd is phosphorylated by uridine-cytidine kinase 2 (UCK2) to form the monophosphate derivative (ECMP), and subsequent phosphorylation reactions yield the actual drug, ECTP, the triphosphate derivative [Shimamoto et al., 2002a, 2002b]. The action mechanism of ECyd (ECTP) is inhibition of RNA polymerases, resulting in the disturbance of various cellular events. Thus, ECyd is thought to be independent of the cell cycle and a type I drug (AUC-dependent). Thus, the encapsulation of ECyd into long-circulating liposomes could enhance its antitumor effect as that of the AUC-dependent type I antitumor drug, Dox.

To design excellent carriers of antitumor drugs, analysis of their antitumor effects based on the physiological model is important. However, such DDS design has rarely been reported. Previously, one of the authors (H. H.) analyzed liposomal Dox based on the model and found that optimization of its release rate is an important factor in the enhancement of the antitumor effect [Tsuchihashi et al., 1999; Harashima et al., 1999].

In this study, the antitumor effect of ECyd was analyzed *in vitro* and *in vivo*. The

antitumor effect of ECyd encapsulated in long-circulating liposomes was also examined. Based on *in vivo* pharmacokinetic (PK)–pharmacodynamic (PD) analyses, a physiological model that could explain its *in vivo* antitumor effect quantitatively was proposed. The model suggested that ECyd followed a time-dependent mechanism of action *in vivo* (in contrast to *in vitro*), and that the availability of ECyd in tumor tissue is highly important. To increase the availability of ECyd, its phospholipid derivatives were synthesized and encapsulated into long-circulating liposomes. These liposomes successfully increased the antitumor effect. These results indicate that the design of carriers of antitumor drugs based on their physiological models is highly important.

2. Materials and methods

2.1. Materials

ECyd was synthesized as described previously [Hattori et al., 1996]. Colon 26 cells were provided by Taiho Pharmaceutical Co. (Tokyo, Japan).

2.2. Chemical synthesis of phospholipid derivatives of ECyd

A mixture of a solution of 3-*sn*-diacylphosphatidylcholine (dipalmitoyl-, distearoyl-, or dioleoyl-phosphatidylcholine, 3.4 mmol) in $CHCl_3$ (50 mL), phospholipase D (PLDP, Asahi Kasei Co., Tokyo, Japan) (60 mg, 10,800 units) and a solution of ECyd (4.54 g, 17

mmol) in sodium acetate buffer (pH 4.5, 200 mM, 25 ml) was stirred at 40 °C for 2.5 h. $CHCl_3$ (60 mL), MeOH (60 mL) and water (10 mL) were added to the resulting mixture, and the organic layer was evaporated. The residue was purified on a silica gel column (33–50% MeOH in $CHCl_3$). The fractions containing the desired product were collected and evaporated. The residue was dissolved in a mixture of $CHCl_3$–MeOH–water (10/5/1), loaded on a WK-20 (Na^+ form) column and eluted using the same mixed solvent. The eluate was evaporated to give DPPECyd, DSPECyd, or DOPECyd as a sodium salt. DPPECyd: yield 52%; mp 206–208°C (decomp.); ^{1}H NMR ($CDCl_3$–CD_3OD (3:1)) 7.96 (d, 1H, H-6, J = 7.6 Hz), 5.94 (d, 1H, ECyd H-1', J = 5.1 Hz), 5.91 (d, 1H, ECyd H-5, J = 7.6 Hz), 5.23 (m, 1H, glycerol H-2), 4.41 (dd, 1H, H-5'a, J = 2.9, 11.7 Hz), 4.2–4.3 (m, 4H, H-2', H-5'b, glycerol CH_2), 4.00 (t, 2H, J = 5.7 Hz, glycerol CH_2), 3.84 (m, 1H, ECyd H-4'), 2.78 (s, 1H, ECyd 3'-ethynyl), 2.28–2.35 (m, 4H, COCH_2 ×2), 1.59 (m, 4H, $COCH_2CH_2$ ×2), 1.26 (m, 48H, pal-CH_2 ×2), 0.88 (t, 6H, J = 6.7 Hz, pal-CH_3 ×2); FAB-MS m/z 920 (MH^+). Anal. calcd. for $C_{46}H_{79}N_3NaO_{12}P\cdot 1/2H_2O$: C, 59.47; H, 8.68; N, 4.52. Found: C, 59.27; H, 8.60; N, 4.03. DSPECyd: yield 45%; mp 222–226 °C (decomp.); ^{1}H NMR ($CDCl_3$–CD_3OD (3:1)) 7.98 (d, 1H, H-6, J = 7.6 Hz), 5.94 (d, 1H, ECyd H-1', J = 4.9 Hz), 5.92 (d, 1H, ECyd H-5, J = 7.6 Hz), 5.23 (m, 1H, glycerol H-2), 4.41 (dd, 1H, H-5'a, J = 3.2, 12.0 Hz), 4.19–4.26 (m, 4H, H-2', H-5'b, glycerol CH_2), 4.00 (t, 2H, J = 5.6 Hz, glycerol CH_2), 3.85 (br, 1H, ECyd H-4'), 2.78 (s, 1H, ECyd 3'-ethynyl), 2.28–2.35 (m, 4H, COCH_2 ×2), 1.59 (m, 4H, $COCH_2CH_2$ ×2), 1.26 (m, 56H, stearoyl-CH_2), 0.88 (t, 6H, J = 6.7 Hz, stearoyl CH_3 ×2); FAB-MS m/z 976 (MH^+). Anal. calcd. for $C_{50}H_{87}N_3NaO_{12}P$: C, 61.52; H, 8.98; N, 4.30. Found: C, 61.39; H, 8.75; N, 4.49. DOPECyd:

yield 56%; mp 208–227 °C (decomp.); ^{1}H NMR ($CDCl_3$–CD_3OD (3:1)) 7.94 (d, 1H, H-6, J = 7.6 Hz), 5.94 (d, 1H, ECyd H-1', J = 4.9 Hz), 5.91 (d, 1H, ECyd H-5, J = 7.6 Hz), 5.30–5.37 (m, 4H, olefinic), 5.22–5.35 (m, 1H, glycerol H-2), 4.41 (dd, 1H, H-5'a, J = 3.4, 12.0 Hz), 4.16–4.26 (m, 4H, H-2', H-5'b, glycerol CH_2), 4.00 (t, 2H, J = 5.7 Hz, glycerol CH_2), 3.69 (br, 1H, ECyd H-4'), 2.76 (s, 1H, ECyd 3'-ethynyl), 2.28–2.35 (m, 4H, COCH_2 ×2), 1.99–2.02 (8H, m, oleoyl-CH_2 ×4), 1.57–1.61 (m, 4H, $COCH_2CH_2$ ×2), 1.24–1.45 (m, 40H, oleoyl-CH_2 ×20), 0.88 (t, 6H, J = 6.8 Hz, oleoyl CH_3 ×2); FAB-MS (neg.) *m/z* 948 $(M–Na)^-$. Anal. calcd. for $C_{50}H_{83}N_3NaO_{12}P$: C, 61.77; H, 8.60; N, 4.32. Found: C, 61.55; H, 8.50; N, 4.33.

2.3. Preparation of liposomes

Liposomes were composed of distearoylphosphatidylcholine, cholesterol, dicetyl phosphate, and 1,2-distearoyl-*sn*-glycero-3-phosphoethanolamine-*N*-[methoxy(polyethylene glycol)-3000] (6:3:1:1 molar ratio). Liposomes encapsulating ECyd or [^{3}H]ECyd were prepared by the hydration method [Szoka and Papahadjopulos, 1980] followed by extrusion (the Mini-Extruder, Avanti polar lipids) through polycarbonate membrane filters (Nuclepore) of 200 nm and 100 nm, twenty-one times for each pore size. The unencapsulated drug was removed by dialysis against saline six times. The encapsulation ratio, determined by radioactivity after the final dialysis, was 5%. Liposomes labeled with [^{3}H]cholesteryl hexadecyl ether (CHE) were prepared by a similar procedure without the dialysis. Liposomes containing a phospholipid derivative of ECyd were composed of egg yolk phosphatidylcholine (EPC), cholesterol, dicetyl phosphate, and

1,2-distearoyl-*sn*-glycero-3-phosphoethanolamine-*N*-[methoxy(polyethylene glycol)-3000] (7:2:1:1 molar ratio). The encapsulation ratio of the phospholipid derivatives was hypothesized as 100%.

2.4. In vitro chemosensitivity test

The growth-inhibitory effects of ECyd on mouse colorectal carcinoma cells were determined by colorimetric assay. Colon 26 cells (5.0×10^4 cells/well) were grown in RPMI-1640 medium with 10% fetal calf serum (100 μl) under a 5% CO_2 / 95% air atmosphere at 37 °C. After 24 hr, the cells were exposed to ECyd at various concentrations for the time periods indicated. The medium containing ECyd was replaced every 12 hr. After exposure to the drug, cells were washed with the medium twice, and then incubated in 100 μl of the medium at 37 °C up to 48 hr after exposure initiation. The medium was removed, 110 μl of TetraColor One (Seikagaku Co., Tokyo, Japan) was added to each well, and the cell cultures were incubated at 37 °C for 3 hr. The absorbance of each well was measured at 450 nm using a Benchmark Plus (BIO-RAD, Hercules, California, USA). The 50% inhibitory concentration (IC_{50}) was determined from the dose–response curve.

2.5. In vivo antitumor activity

Colon 26 cells (1×10^7 cells/mouse) were transplanted hypodermically into 5-week-old male BALB/c mice on day 0. ECyd, or liposomes encapsulating ECyd, were intravenously administered to tumor-bearing BALB/c mice on days 5 and 10, or on day 8.

Tumors were collected on day 15 from ether-anesthetized mice, and the averaged volumes of tumors in the administered mice were calculated. The inhibition ratio (IR) was calculated using the equation below:

$$\text{IR}\ (\%) = \left(1 - \frac{\text{mean tumor volume of treated group}}{\text{mean tumor volume of control group}} \right) \times 100 \qquad \text{(eq. 1)}$$

2.6. Pharmacokinetics of free ECyd

Colon 26 cells (1 X 10^7 cells/mouse) were transplanted hypodermically into 5-week-old male BALB/c mice on day 0. [^{3}H]ECyd was intravenously administered to tumor-bearing BALB/c mice. Blood and tumor were collected from ether-anesthetized mice. 100 μl of blood and 1 ml of Soluene-350 (Perkin Elmer, Wellesley, MA, USA) were mixed and incubated at 50 °C for 15–30 min, decolorized with 30% hydrogen peroxide, and mixed with aqueous counting scintillant (Hionic-Fluor, Perkin Elmer). The mixture was kept at 4 °C overnight. 100–200 mg of the collected tumor was solubilized in 1 ml of Soluene-350 by incubation at 50 °C for 2–4 hr, and mixed with Hionic-Fluor. The mixture was kept at 4 °C overnight. ^{3}H-radioactivity was counted on a liquid scintillation counter.

2.7. Pharmacokinetics of liposomes

Liposomes labeled with [^{3}H]CHE or liposomes encapsulating [^{3}H]ECyd were intravenously administered to tumor-bearing BALB/c mice, and the time courses of the

concentration in blood and the amount in tumor were measured as described above.

2.8. Computational simulations

The pharmacokinetic data were analyzed using SAAM II (SAAM Institute, Seattle, WA, USA) and Stella (High Performance Systems, Hanover, NH, USA) software.

The mass balance equations for free ECyd (Scheme 1A) are as follows:

Blood $V_{b,f} \bullet dC_{b,f}/dt = k_{21} \bullet X_{ti,f} + k_{31} \bullet V_{tu,f} \bullet C_{tu,f} - (k_{10} + k_{12} + k_{13}) \bullet V_{b,f} \bullet C_{b,f}$ (eq. 2)

Tumor $V_{tu,f} \bullet dC_{tu,f}/dt = k_{13} \bullet V_{b,f} \bullet C_{b,f} - k_{31} \bullet V_{tu,f} \bullet C_{tu,f}$ (eq. 3)

Tissue $dX_{ti,f}/dt = k_{12} \bullet V_{b,f} \bullet C_{b,f} - k_{21} \bullet X_{ti,f}$ (eq. 4)

The mass balance equations for free ECyd upon liposomal ECyd injection (Scheme 1A) are as follows:

Blood $V_{b,f} \bullet dC_{b,f}/dt = k_{21} \bullet X_{ti,f} + k_{31} \bullet V_{tu,f} \bullet C_{tu,f} - (k_{10} + k_{12} + k_{13}) \bullet V_{b,f} \bullet C_{b,f} + (k_{rel,blood,fast} + k_{rel,blood,slow}) \bullet V_{b,lipo} \bullet C_{b,lipo}$ (eq. 5)

Tumor $V_{tu,f} \bullet dC_{tu,f}/dt = k_{13} \bullet V_{b,f} \bullet C_{b,f} - k_{31} \bullet V_{tu,f} \bullet C_{tu,f} + k_{rel,tumor} \bullet V_{tu,lipo} \bullet C_{tu,lipo}$ (eq. 6)

Tissue $dX_{ti,f}/dt = k_{12} \bullet V_{b,f} \bullet C_{b,f} - k_{21} \bullet X_{ti,f}$ (eq. 4)

The mass balance equations for liposomal ECyd upon liposomal ECyd injection (Scheme 1A) are as follows:

Blood $V_{b,lipo} \bullet dC_{b,lipo}/dt = k_{54} \bullet V_{tu,lipo} \bullet C_{tu,lipo} - (k_{40} + k_{45} + k_{rel,blood,fast} + k_{rel,blood,slow}) \bullet V_{b,lipo} \bullet C_{b,lipo}$

(eq. 7)

Tumor $V_{tu,lipo} \bullet dC_{tu,lipo}/dt = k_{45} \bullet V_{b,lipo} \bullet C_{b,lipo} - (k_{54} + k_{rel,tumor}) \bullet V_{tu,lipo} \bullet C_{tu,lipo}$ (eq. 8)

$V_{b,f}$ and $V_{tu,f}$ represent the volumes of distribution for free ECyd in the blood and tumor compartments, respectively. $V_{b,lipo}$ and $V_{tu,lipo}$ represent the volumes of distribution for liposomal ECyd in the blood and tumor compartments, respectively. $C_{b,f}$, $C_{tu,f}$, $C_{b,lipo}$, and $C_{tu,lipo}$ represent the free and liposomal ECyd concentrations in the blood and tumor compartments. $X_{ti,f}$ represents amount of free ECyd in the tissue compartment. k_{10} and k_{40} represent the elimination constants for free and liposomal ECyd, respectively. k_{12}, k_{13}, k_{21}, k_{31}, k_{45}, and k_{54} represent the distribution rate constants. $k_{rel,tumor}$ represents the ECyd release rate constant in the tumor compartment. $k_{rel,blood,fast}$ and $k_{rel,blood,slow}$ represent the fast and slow ECyd release rate constants in the blood compartment, respectively.

3. Results

3.1. AUC-dependence of the cytotoxic effects of ECyd in vitro

The cytotoxic effects of ECyd on mouse colorectal carcinoma cells (Colon 26 cells) were determined by MTT assay. Exposure time was altered (4, 12, 24 and 48 h), and IC_{50} values were determined for each exposure time. As shown in Supplementary Table 1, the IC_{50} values decreased as the treatment time increased. AUC, the product of the exposure time and

the IC_{50} values obtained, were similar for each condition. These results were in agreement with the hypothesis that ECyd is a cell cycle-independent antitumor drug, since ECyd inhibits RNA synthesis. In addition, these results suggest that the antitumor effect of ECyd would be independent of the administration schedule *in vivo*.

3.2. Pharmacokinetics of ECyd

[^{3}H]ECyd was intravenously administered to tumor-bearing BALB/c mice and radioactivity in blood and tumors was determined (Fig. 2A and B). The amounts in blood and tumors, relative to the injected [^{3}H]ECyd, were similar when various amounts of [^{3}H]ECyd were injected (data not shown), indicating the linearity of the drug disposition under our experimental conditions. Importantly, ECyd was cleared rapidly from blood.

3.3. AUC-independence of the antitumor effects of ECyd in vivo

Various doses of ECyd were then intravenously administered to tumor-bearing BALB/c mice on days 5 and 10 (double administration), or day 8 (single administration). Tumors were collected on day 15 and the IR values were determined. In contrast to the expectations based on the *in vitro* cytotoxic effect (Supplementary Table 1), the antitumor effect of ECyd was schedule-dependent. As shown in Table 1 (Experiment 1) and Fig. 3A, double administration of ECyd inhibited tumor growth more effectively than single administration of the same total dose of ECyd. For example, the IR of a single 3.0 mg/kg injection was 48%, and that of double 1.5 mg/kg injections was 86%. Since the PK of ECyd

was linear under the experimental conditions, as described above, these results indicate type II-like AUC-independence of the antitumor effects of ECyd *in vivo*.

3.4. PK–PD modeling of ECyd

PK parameters were obtained by curve-fitting based on the three-compartment model shown in Scheme 1A (see "Free ECyd") and the actual ECyd dose data in blood and tumor tissue (Fig. 2A and B), according to the equations described in the Materials and Methods section. The PK parameters obtained are shown in Table 2. The linearity of the ECyd disposition under these conditions was observed, and the same values of the parameters were used in the following simulations.

To explain the fact that the antitumor effect of ECyd was AUC-dependent *in vitro* and AUC-independent *in vivo* (Supplementary Table 1 and Table 1, Experiment 1), the presence of a minimum effective concentration (C_{min}) was introduced as a new parameter. We hypothesized that ECyd can exert antitumor effect only when free concentration of ECyd exceeds the C_{min} in tumor tissue (Scheme 1B). However, since we could not measure the C_{min}, we estimated the C_{min} based on the simulation as explained below. The putative C_{min} value was changed in the simulation, and the effective time within which the ECyd concentration in the tumor was above C_{min} was calculated for each C_{min} value. We then examined the curve-fitting of calculated effective times and the actually observed IR values, using the following equation

$$IR = \frac{E_{max} \times t^r}{t_{50}^r + t^r} \qquad \text{(eq. 9)}$$

where E_{max}, t, and t_{50} represent the maximum efficacy (set as 100%), effective time, and 50% inhibitory time, respectively. In the case of double administration, the calculated effective time was doubled. As shown in Fig. 3B, the IR data of the single and double administration experiments fitted well as the function of effective time when C_{min} was set at 61.1 fmol/g (the t_{50} and r values were calculated as 147.5 hr and 2.9, respectively). Thus, the threshold value C_{min} could well explain the *in vivo* antitumor effects of ECyd.

3.5. The antitumor effects of liposomal ECyd in vivo

The results shown above suggest that the antitumor effect of ECyd would be enhanced by encapsulation into long-circulating liposomes and prolonged exposure of tumor cells to ECyd above C_{min}. PEGylated liposomes containing ECyd were then prepared. The encapsulation ratio was 5%. Liposomal ECyd was administered as free ECyd to tumor-bearing BALB/c mice on days 5 and 10 (double administration) or on day 8 (single administration). Unexpectedly, however, liposomal ECyd inhibited tumor growth less efficiently than unencapsulated ECyd, irrespective of the injection schedule (Table 1, Experiment 2).

3.6. PK–PD modeling of liposomal ECyd

To determine the reason the liposomal ECyd was unexpectedly less effective than free ECyd, the PK of liposomal ECyd was analyzed. Both the liposome membrane and ECyd were traced after administration. As shown in Fig. 2C, ~10% of liposomes modified with PEG were present in blood after 24 hr, showing the nature of long-circulating liposomes. Nearly 10% of the injected liposomes reached tumor tissue at 24 hr (Fig. 2D). The disposition of total ECyd, which includes released and liposomal ECyd, is also shown in Figures 2C and D. The amounts of total ECyd in blood and tumor were not identical to those of liposomes, indicating the release of ECyd from liposomes. We had hypothesized that ECyd released in and near the tumor would accumulate in the tumor. However, the amount of ECyd was half that of the liposomes in the tissue. As described above, the liposomal ECyd injection was less effective than free ECyd injection (Table 2, Experiments 1 and 2). Taken together, these results suggest that the free ECyd concentration in the tumor was lower for the liposomal ECyd injection than for the free ECyd injection.

A PK model containing liposomal and free ECyd (Scheme 1A) was then constructed, and curve-fitting was carried out based on this model and the actual data. First, the data on [^{3}H]CHE-liposome, which correspond to the disposition of the liposome itself, were analyzed according to the two-compartment model consisting of blood and tumor compartments, since the change in disposition of the liposomes could be approximated by elimination by RES and distribution in the tumor. Data on [^{3}H]ECyd were analyzed using the three-compartment model. Based on the PK parameters determined by the simulations, latency (encapsulation efficiency *in vivo*) were calculated (Supplementary Fig. 1). The latency curve was a

combination of two functions that appear to reflect fast and slow releases of ECyd from liposomes. These two release rates might be due to the presence of multilamellar and unilamellar vesicles. The release rate constant ($k_{rel,tumor}$) was calculated to be 0.02 hr^{-1}, a three-fold higher value than the rate constant of the slow release in blood ($k_{rel,blood,slow}$) (Table 2 and Scheme 1A). Effective times for which tumor cells were exposed to free ECyd above the C_{min} value (61.1 fmol/g) obtained from the free ECyd injection data and the simulation were calculated (Fig. 2A and B, and Fig. 3B). The IR data from the single injections of the liposomal ECyd were on/near the effective time–IR curve (Fig. 3C, circles). In contrast, data from the double injections of the liposomal ECyd were out of the curve (triangles). It has been reported that second injections of PEG-liposomes are cleared rapidly from blood (accelerated blood clearance (ABC) phenomenon) [Dams et al., 2000; Laverman et al., 2001; Ishida et al., 2003a, 2003b]. The actual effective times for double administration might be half of those in the simulation, owing to the ABC phenomenon of the second injection of liposomes. The insufficient antitumor activity and the simulation suggest that the PEG-liposomes did not deliver free ECyd to the tumor more efficiently than the free ECyd injection. These results indicate that the availability of "free" ECyd in the tumor tissue is important.

3.7. Enzymatic synthesis of the phospholipid derivatives of ECyd

The simulations based on the PK data of free and liposomal ECyd prompted the use of ECyd-phospholipid derivatives that may improve delivery to the tumor and availability in the tumor. Three ECyd-phospholipid derivatives were prepared, in which phospholipids were

attached to ECyd via the 5'-phosphate (Fig. 1). The ECyd-phospholipid derivatives have affinity to the cell membrane, and might move from liposomes to the cell membrane. The derivatives on the inner membrane might release the monophosphate derivative of ECyd (ECMP) into the cytosol of tumor cells. This might overcome the important barriers of uptake by transporter(s) and 5'-phosphorylation by UCK2. Controlled release of ECMP from the phospholipid derivatives might be useful, since the first phosphorylation of nucleoside analogs is a determining factor for their efficacy [Matsuda and Sasaki, 2004].

An enzymatic method was previously developed for the preparation of phospholipid derivatives of nucleosides from a nucleoside and a phosphatidylcholine by a one-step reaction, in which phospholipase D-catalyzed transphosphatidylation, namely, the regiospecific transfer reaction of the phosphatidyl residue from a phosphatidyalcholine to the 5'-hydroxyl of a nucleoside, was used [Shuto et al., 1987]. The phospholipid derivatives of ECyd used in this study were effectively synthesized by this method.

3.8. The improved antitumor effects of liposomes containing ECyd-phospholipid derivative

Liposomes containing ECyd-phospholipid were administered to tumor-bearing mice. As shown in Table 1 (Experiment 3), liposomal DPPECyd inhibited tumor growth by 55% while free ECyd inhibited it by 35%. In addition, DPPECyd did not cause body weight change, an indicator of side effects. Liposomal DSPECyd was most effective and inhibited tumor growth by 68%, although it caused a decrease in body weight, suggesting severe side effects. In contrast, liposomal DOPECyd showed tumor growth inhibition similar to that by

free ECyd. These results indicate that ECyd-phospholipid derivatives could enhance the antitumor activity of ECyd by increasing its availability in tumor tissue.

4. Discussion

The antitumor effect of ECyd was AUC-dependent *in vitro* and time-dependent *in vivo* (Supplementary Table 1 and Table 1, Experiment 1). It appears that the efficacy of ECyd actually depends on both concentration and time, and that apparent dependency changes with the experimental conditions. ECyd is taken up into cells by transporters [Endo et al., 2007] and phosphorylated by UCK2 to ECMP [Shimamoto et al., 2002a, 2002b]. The actual drug, ECTP, is formed by subsequent phosphorylation reactions from ECMP, but the first phosphorylation reaction would be most important for the efficacy of ECyd. The incorporated ECyd is excreted from cells by transporter(s). When measured *in vitro*, the influx clearance of ECyd was lower than its efflux clearance, suggesting the presence of efflux transporter(s) (data not shown). However, it is possible that the phosphorylated forms of ECyd are hardly excreted. The conversion of ECyd to ECMP by UCK2 would not occur substantially at low extracellular ECyd concentrations because of the efflux transporter(s). Thus, an amount of ECyd higher than a certain “threshold” would be required for the cytotoxic effect, and totally synthesized ECTP should be dependent on both its extracellular ECyd concentration and exposure time. This could be a reason for the AUC-dependency of ECyd *in vitro* (Supplementary Table 1).

Considering that the uptake of ECyd and its conversion to ECMP are carried out by enzymes, saturation of their activities can be easily assumed. A highly excessive amount of ECyd would not lead to dose-dependent accumulation of ECTP. Therefore, dose-dependency of the efficacy would be present within a certain concentration range. *In vitro*, extracellular ECyd concentration is thought to be constant during the exposure time, due to a lack of clearance from the medium. On the other hand, the half life of ECyd in blood was very short, and ECyd concentration in the tumors varied, increasing and then decreasing (Fig. 2A and B). Tumor cells near blood vessels, in particular, would be exposed transiently to a high concentration of ECyd. In this study, a putative concentration value, C_{min}, was proposed in the simulation to explain the schedule-dependency of the ECyd antitumor effect *in vivo*. The calculated effective time based on this value could explain the efficacy of free and liposomal ECyd (Fig. 3B and C). Since the uptake, excretion, and phosphorylation of ECyd are conducted by enzymes, as described above, a simple linear correlation between AUC and IR would not be present. In such cases, the concept of C_{min} might be a good parameter to explain the efficacy of other drugs.

Calculation of release rates of ECyd from PEG-liposomes showed the presence of two values (Table 2 and Supplementary Fig. 1). The $k_{rel,blood,fast}$ and $k_{rel,blood,slow}$ values were calculated to be 0.52 and 0.006 hr^{-1}, respectively. These two release rates could be attributed to the possible presence of two fractions of liposomes, multilamellar and unilamellar vesicles. The fast rates would reflect ECyd release from the outermost aqueous phase. The release rate constant in tumor tissue ($k_{rel,tumor}$) was calculated to be a three-fold higher value of the rate

constant of the slow release in blood ($k_{rel,blood,slow}$). This suggests that certain collapse mechanism(s) of liposomes, such as phagocytization by macrophages, are present near the tumor. Different drug release rates in blood and tumor are suggested in this study, although the same release rates were hypothesized in previous studies by Harashima et al. [Tsuchihashi et al., 1999; Harashima et al., 1999].

Single and double administration of ECyd encapsulated in PEG-liposomes was less effective than injection of ECyd alone (Table 1, Experiments 1 and 2). PK analyses indicate that the apparent ECyd concentration in tumor was higher for liposomal ECyd than for ECyd alone (Fig. 2B and D). However, the simulation based on the model shown in Scheme 1A suggests that ~75% of ECyd was present in the encapsulated form in tumor tissue (data not shown). This would result in the reduction of the availability of ECyd in the tumor for liposomal ECyd. Thus, it should be emphasized that disposition in a target site, but not in blood, is important for the design of the optimal carrier of a drug.

The simulations based on the PK data of free and liposomal ECyd prompted the use of ECyd-phospholipid derivatives for improvement of the trafficking to and availability in the tumor tissue. Indeed, the liposomes containing DPPECyd and DSPECyd showed increased antitumor effects compared with free ECyd (Table 1, Experiment 3). In contrast, liposomal DOPECyd showed tumor growth inhibition similar to that by free ECyd. Thus, alteration in chain-length might make controlled release possible. The order of IR was DSP > DPP > DOP. This order agrees with that of instability of phospholipids in liposomes. The absence of the unsaturated C–C bond and the short carbon chain destabilizes liposomes and consequently

leads to the release of the ECyd-phospholipids and transfer to the plasma membrane of tumor cells. DSPECyd could stay in liposomes, and the controlled release of this ECyd derivative could produce the actual drug ECTP most effectively. Additionally, liposomal DSPECyd caused a decrease in body weight, suggesting side effects, although liposomal DPPECyd and DOPECyd did not. The alteration in chain-length could also control toxicity. The other advantages of the encapsulation of phospholipid-derivatives of ECyd were improved encapsulation ratio (from 5% for ECyd to 100% for the derivatives) and alteration in incorporation pathways, avoiding influx transporters.

In this study, dispositions of free and liposomal ECyd were compared *in vivo*, and the establishment of C_{min} value and resulting effective time in simulation could explain the efficacy of ECyd drugs. It is probable that the effects of type II antitumor drugs that depend on exposure time and the cell cycle can be predicted by simple modeling and calculation using this C_{min} value. An important conclusion is that the encapsulation of ECyd-phospholipid derivatives into long-circulating liposomes could enhance antitumor activity, possibly due to improved availability in the target tissue.

Acknowledgement

This work was supported in part by Grants-in-Aid from the Ministry of Education, Culture, Sports, Science and Technology of Japan, and from the Japan Society for the Promotion of Science.

References

Allen, T. M., Hansen, C., Martin, F., Redemann, C., Yau-Yong, A., 1991. Liposomes containing synthetic lipid derivatives of poly(ethylene glycol) show prolonged circulation half-times in vivo. Biochim. Biophys. Acta, 1066, 29-36.

Blume, G., Cevc, G., 1990. Liposomes for the sustained drug release *in vivo*. Biochim. Biophys. Acta, 1029, 91-97.

Dams, E. T. M., Laverman, P., Oyen, W. J. G., Storm, G., Scherphof, G. L., Van der Meer, J. W. M., Corstens, F. H. M., Boerman, O. C., 2000. Accelerated blood clearance and altered biodistribution of repeated injections of sterically stabilized liposomes. J. Pharmacol. Exp. Ther., 292, 1071–1079.

Endo, Y., Obata, T., Murata, D., Ito, M., Sakamoto, K., Fukushima, M., Yamasaki, Y., Yamada, Y., Natsume, N., Sasaki, T., 2007. Cellular localization and functional characterization of the equilibrative nucleoside transporters of antitumor nucleosides. Cancer Sci., 98, 1633-1637.

Harashima, H., Iida, S., Urakami, Y., Tsuchihashi, M., Kiwada, H., 1999. Optimization of antitumor effect of liposomally encapsulated doxorubicin based on simulations by pharmacokinetic/pharmacodynamic modeling. J. Control. Release, 61, 93-106.

Hattori, H., Tanaka, M., Fukushima, M., Sasaki, T., Matsuda, A., 1996. Nucleosides and nucleotides. 158. 1-(3-*C*-ethynyl-β-D-ribo-pentofuranosyl)-cytosine, 1-(3-*C*-ethynyl-β-D-ribo-pentofuranosyl)uracil, and their nucleobase analogues as new potential multifunctional antitumor nucleosides with a broad spectrum of activity. J. Med.

Chem., 39, 5005-5011.

Ishida, T., Maeda, R., Ichihara, M., Irimura, K., Kiwada, H., 2003a. Accelerated clearance of PEGylated liposomes in rat after repeated injection. J. Control. Release, 88, 35–42.

Ishida, T., Masuda, K., Ichikawa, T., Ichihara, M., Irimura, K., Kiwada, H., 2003b. Accelerated clearance of a second injection of PEGylated liposomes in mice. Int. J. Pharm., 255, 167–174.

Klibanov, A. L., Maruyama, K., Torchilin, V. P., Huang, L., 1990. Amphipathic polyethyleneglycols effectively prolong the circulation time of liposomes. FEBS Lett., 268, 235-237.

Laverman, P., Carstens, M. G., Boerman, O. C., Dams, E. T. M., Oyen, W. J. G., Rooijen, N. V., Corstens, F. H. M., Storm, G., 2001. Factors affecting the accelerated blood clearance of polyethylene glycol-liposomes upon repeated injection. J. Pharmacol. Exp. Ther., 298, 607–612.

Matsuda, A., Sasaki, T., 2004. Antitumor activity of sugar-modified cytosine nucleosides. Cancer Sci., 95, 105-111.

Ozawa, S., Sugiyama, Y., Mitsuhashi, Y., Kobayashi, T., Inaba, M., 1988. Cell killing action of cell cycle phase-non-specific antitumor agents is dependent on concentration-time product. Cancer Chemother Pharmacol., 21, 185-190.

Ozawa, S., Sugiyama, Y., Mitsuhashi, J., Inaba, M., 1989. Kinetic analysis of cell killing effect induced by cytosine arabinoside and cisplatin in relation to cell cycle phase specificity in human colon cancer and chinese hamster cells. Cancer Res., 49, 3823-3828.

Papahadjopoulos, D., Allen, T. M., Gabizon, A., Mayhew, E., Matthay, K., Huang, S. K.,,Lee, K. D., Woodle, M. C., Lasic, D. D., Redemann, C., Martin, F. J., 1991. Sterically stabilized liposomes: improvements in pharmacokinetics and antitumor therapeutic efficacy. Proc. Natl. Acad. Sci. USA, 88, 11460-11464.

Shimamoto, Y., Kazuno, H., Murakami, Y., Azuma, A., Koizumi, K., Matsuda, A., Sasaki, T., Fukushima, M., 2002a. Cellular and biochemical mechanisms of the resistance of human cancer cells to a new anticancer ribo-nucleoside, TAS-106. Jpn. J. Cancer Res., 93, 445-452.

Shimamoto, Y., Koizumi, K., Okabe, H., Kazuno, H., Murakami, Y., Nakagawa, F., Matsuda, A., Sasaki, T., Fukushima, M., 2002b. Sensitivity of human cancer cells to the new anticancer ribo-nucleoside TAS-106 is correlated with expression of uridine-cytidine kinase 2. Jpn. J. Cancer Res., 93, 825-833.

Shimoyama, M., 1975. Cytocidal action of anticancer antigens: evaluation of the sensitivity of cultured animal and human cancer cells. Bibliotheca Haematologica, 40, 711-722.

Shuto, S., Ueda, S., Imamura, S., Fukukawa, K., Matsuda, A., Ueda, T., 1987. A facile one-step synthesis of 5'-phosphatidylnucleosides by an enzymatic two-phase reaction. Tetrahedron Lett., 28, 199-202.

Szoka, F. C., Papahadjopulos, D., 1980. Comparative properties and methods of preparation of lipid vesicles (liposomes). Ann. Rev. Biophys. Bioeng., 9, 467-508.

Tabata, S., Tanaka, M., Endo, Y., Obata, T., Matsuda, A., Sasaki, T., 1997. Anti-tumor mechanisms of 3'-ethynyluridine and 3'-ethynylcytidine as RNA synthesis inhibitors:

development and characterization of 3'-ethynyluridine-resistant cells. Cancer Lett., 116, 225-231.

Takatori, S., Tsutsumi, S., Hidaka, M., Kanda, H., Matsuda, A., Fukushima, M., Wataya, Y., 1998. The characterization of cell death induced by 1-(3-*C*-ethynyl-β-D-ribo-pentofuranosyl) cytosine (ECyd) in FM3A cells. Nucleosides Nucleotides, 17, 1309-1317.

Takatori, S., Kanda, H., Takenaka, K., Wataya, Y., Matsuda, A., Fukushima, M., Shimamoto, Y., Tanaka, M., Sasaki, T., 1999. Antitumor mechanisms and metabolism of the novel antitumor nucleoside analogues, 1-(3-*C*-ethynyl-β-D-ribo-pentofuranosyl)cytosine and 1-(3-*C*-ethynyl-β-D-ribo-pentofuranosyl)uracil. Cancer Chemother. Pharmacol., 44, 97-104.

Tsuchihashi, M., Harashima, H., Kiwada, H., 1999. Development of a pharmacokinetic/pharmacodynamic (PK/PD)-simulation system for doxorubicin in long circulating liposomes in mice using peritoneal P388. J. Control. Release, 61, 9-19.

Vaage, J., Donovan, D., Mayhew, E., Uster, P., Woodle, M., 1993. Therapy of mouse mammary carcinomas with vincristine and doxorubicin encapsulated in sterically stabilized liposomes. Int. J. Cancer, 54, 959-964.

Legends for Figures and Schemes

Figure 1. Chemical structures of ECyd and its phospholipid derivatives.

Figure 2. (A and B) Concentration of ECyd in blood (A) and tumor (B) upon injection of free ECyd. (C and D) Concentrations of ECyd (open circles) and liposomes (closed circles) in blood (C) and tumor (D) upon injection of liposomal ECyd. The curves are drawn by the simulations based on the PK model shown in Scheme 1A. Bars represent SD.

Figure 3. (A and B) Relationships between administration dose and IR (A) and between effective time and IR (B) upon injection of free ECyd. (C) Relationship between effective time and IR upon administration of liposomal ECyd. (A) The data shown in Table 1 (Experiment 1) are plotted. (B) The effective time was calculated when the C_{min} value was set as 61.1 fmol/g. The data shown in panel A are replotted using the effective time as the horizontal axis. (C) The data shown in Table 1 (Experiment 2) are plotted using the effective time calculated when the C_{min} value was set as 61.1 fmol/g as the horizontal axis. Circles and triangles represent the data obtained from the single and double injections, respectively. Bars represent SD. The fitted curves in panel A were drawn, using the following equation

$$IR = \frac{E_{max} \times D^r}{D_{50}^r + D^r} \qquad \text{(eq. 10)}$$

where E_{max}, D, and D_{50} represent the maximum efficacy (set as 100%), dose, and 50% inhibitory dose, respectively. The fitted curve in panel B was drawn according to equation 9 in the text, and the same curve was imposed in panel C to show that the IR data of the liposomal ECyd were on/near the effective time–IR curve only for the single injections.

Scheme 1. (A) Pharmacokinetic model of free and liposomal ECyd and (B) explanatory drawing of C_{min} and effective time. (B) Hypothetical free concentration of a drug in target tissue.

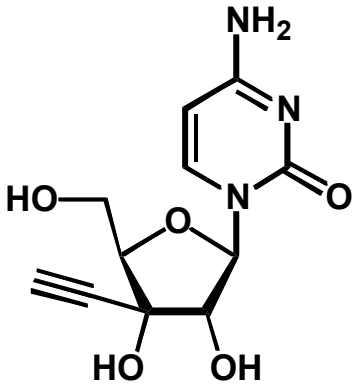

ECyd

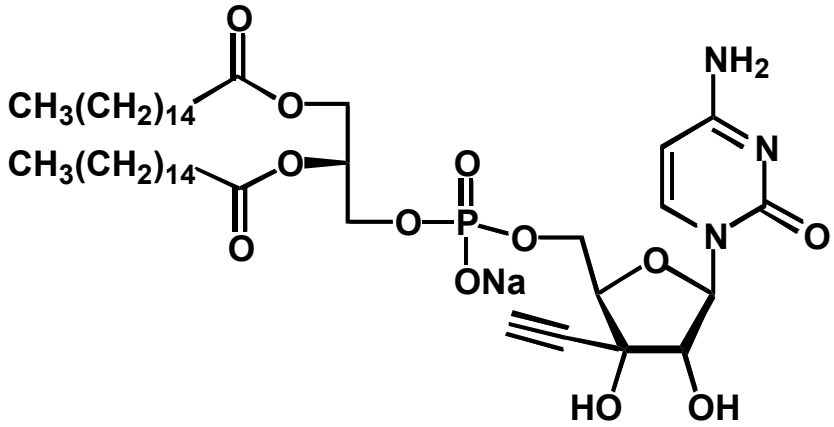

DPPECyd

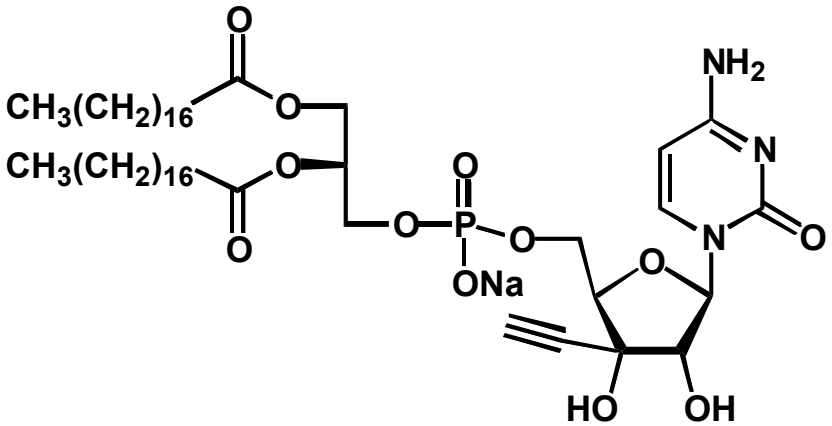

DSPECyd

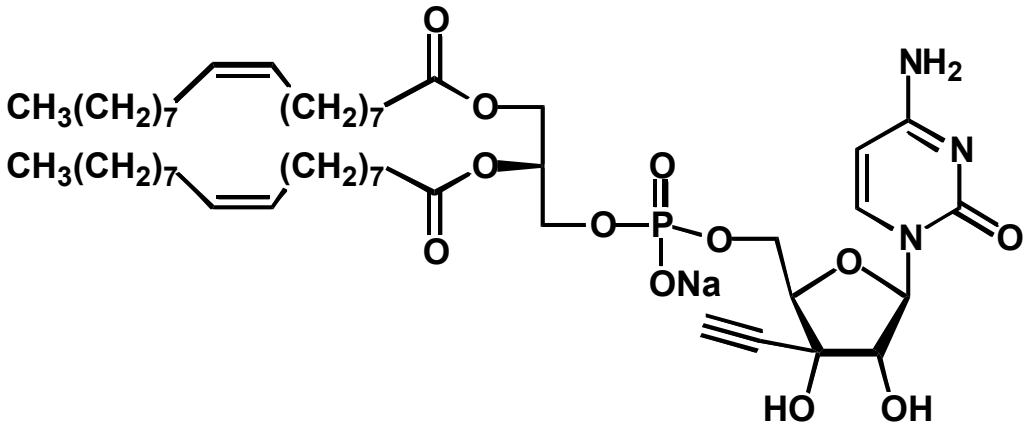

DOPECyd

Fig. 1

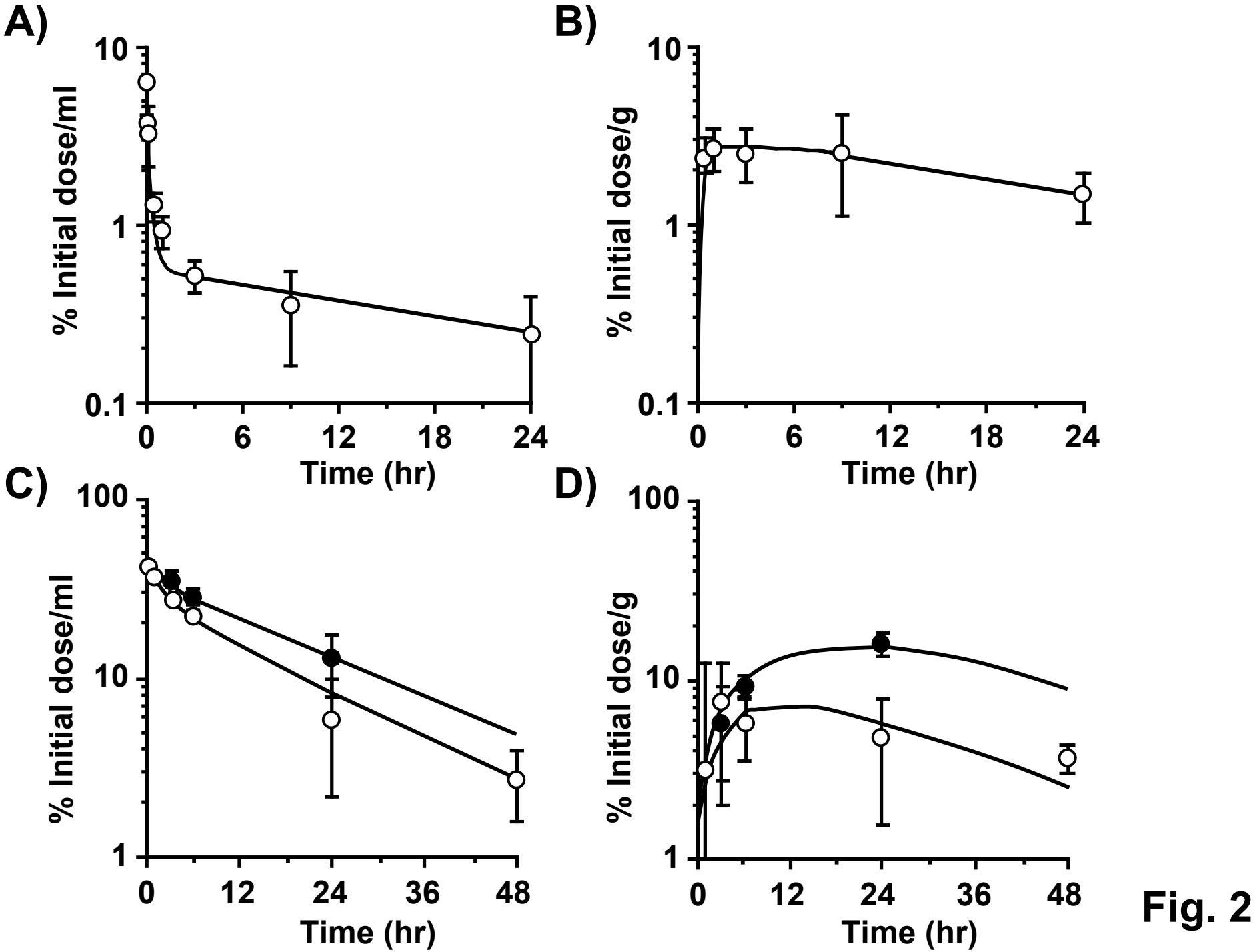
A)
% Initial dose/ml
10
1
0.1
0
6
12
18
24
Time (hr)
B)
% Initial dose/g
10
1
0.1
0
6
12
18
24
Time (hr)
C)
% Initial dose/ml
100
10
1
0
12
24
36
48
Time (hr)
D)
% Initial dose/g
100
10
1
0
12
24
36
48
Time (hr)

Fig. 2

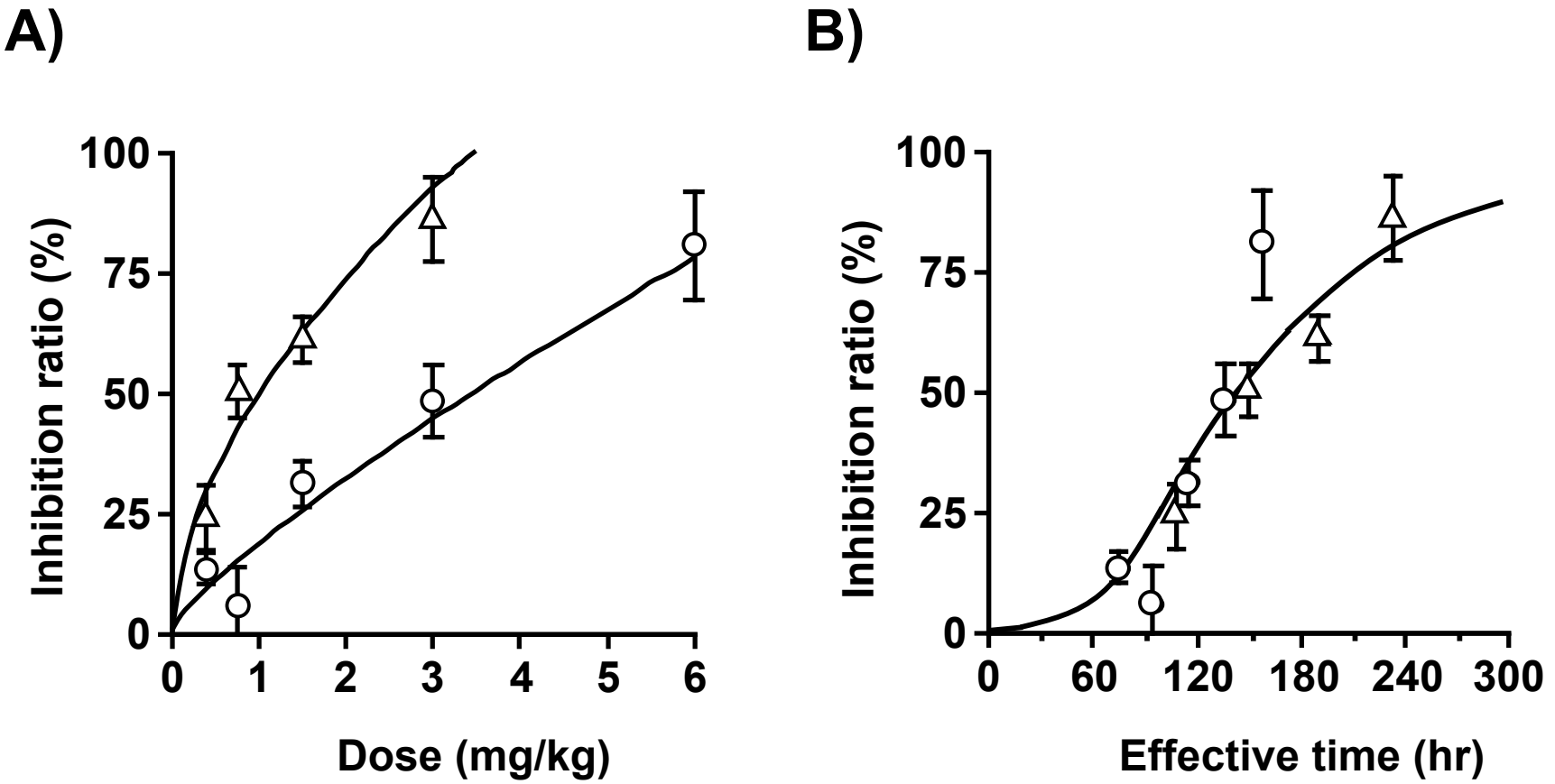
A)
B)
Inhibition ratio (%)
100
75
50
25
0
0
1
2
3
4
5
6
Dose (mg/kg)
Inhibition ratio (%)
100
75
50
25
0
0
60
120
180
240
300
Effective time (hr)

Fig. 3A, B

C)

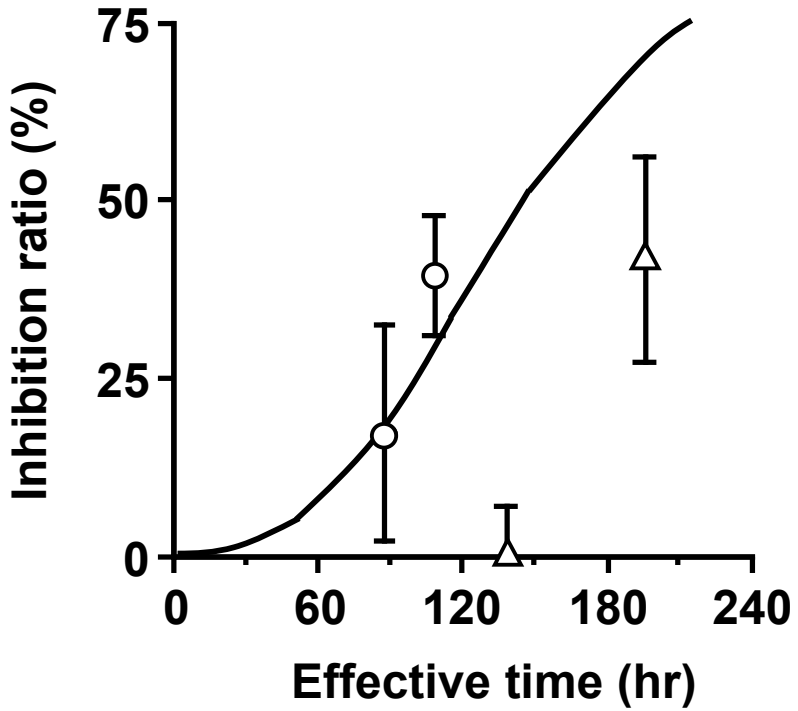

Fig. 3C

Table 1

Table 1 Inhibition of tumor growth by administration of Ecyd and its derivatives.

Drug	Dose [a] (mg/kg)	No. of death	BWC (%) [b] on day 15	IR (%) [c] on day 15
Experiment 1				
None	0.00	0/4	-2.0	NA [d]
ECyd	0.38	0/4	1.3	13.5
i.v. on day 8	0.75	0/4	15.0	5.9
	1.50	0/4	12.9	31.1
	3.00	0/4	7.3	48.2
	6.00	0/4	10.4	80.7
ECyd	0.19 X 2	0/4	5.2	24.1
i.v. on days 5 & 10	0.38 X 2	0/4	10.0	50.4
	0.75 X 2	0/4	7.9	61.2
	1.50 X 2	0/4	13.6	85.9
Experiment 2				
None	0.00	0/4	8.4	NA [d]
Liposome	0.00	0/4	9.4	NA [d]
Liposomal ECyd	1.50	0/4	8.9	17.2
i.v. on day 8	3.00	0/4	8.5	39.5
Liposomal ECyd	0.75 X 2	0/4	8.9	-1.0
i.v. on days 5 & 10	1.50 X 2	0/4	8.5	41.5
Experiment 3				
None	0.00	0/5	-15.1	NA [d]
ECyd	3.00	0/5	-2.5	35.0
i.v. on day 8				
Liposomal DPPECyd	3.00	0/5	-2.7	55.2
i.v. on day 8				
Liposomal DSPECyd	3.00	0/5	-20.9	68.2
i.v. on day 8				
Liposomal DOPECyd	3.00	0/5	-2.2	32.4
i.v. on day 8				

[a] As ECyd.

[b] Body weight change calculated according to the following formula:

BWC (%) = [(body weight on day 15) – (body weight on day 0)] / (body weight on day 0) × 100

[c] IR on the basis of tumor volume was calculated according to the following formula:

IR (%) = [1 – (mean tumor volume of treated group) / (mean tumor volume of control group)] × 100

[d] Not applicable.

Table 2 Pharmacokinetic parameters obtained by simulations

Pharmacokinetic Parameters for Free ECyd	
V_{ECyd}(ml)	16.9
k_{10}(hr^{-1})	0.34
k_{12}(hr^{-1})	3.23
k_{21}(hr^{-1})	0.39
k_{13}(hr^{-1})	0.02
k_{31}(hr^{-1})	0.33
Pharmacokinetic Parameters for Liposomes	
$V_{Liposome}$(ml)	2.14
k_{40}(hr^{-1})	0.04
k_{45}(hr^{-1})	0.003
k_{54}(hr^{-1})	0.06
Pharmacokinetic Parameters for Liposomal ECyd	
$k_{rel,blood,fast}$(hr^{-1})	0.52
$k_{rel,blood,slow}$(hr^{-1})	0.006
$k_{rel,tumor}$(hr^{-1})	0.02

A)

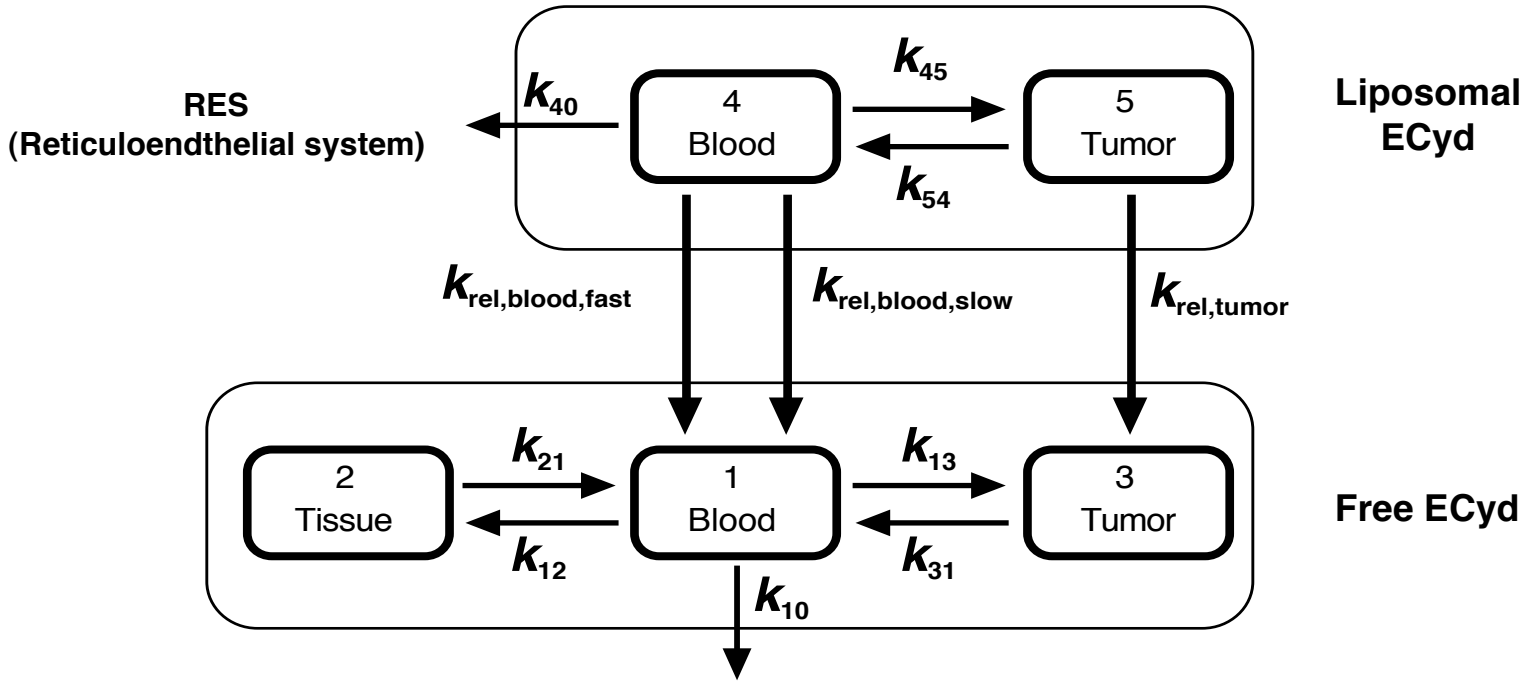
RES
(Reticuloendthelial system)
k_{40}
4
Blood
k_{45}
5
Tumor
k_{54}
Liposomal
ECyd
$k_{rel,blood,fast}$
$k_{rel,blood,slow}$
$k_{rel,tumor}$
2
Tissue
k_{21}
k_{12}
1
Blood
k_{13}
k_{31}
3
Tumor
k_{10}
Free ECyd

Scheme 1A

B)

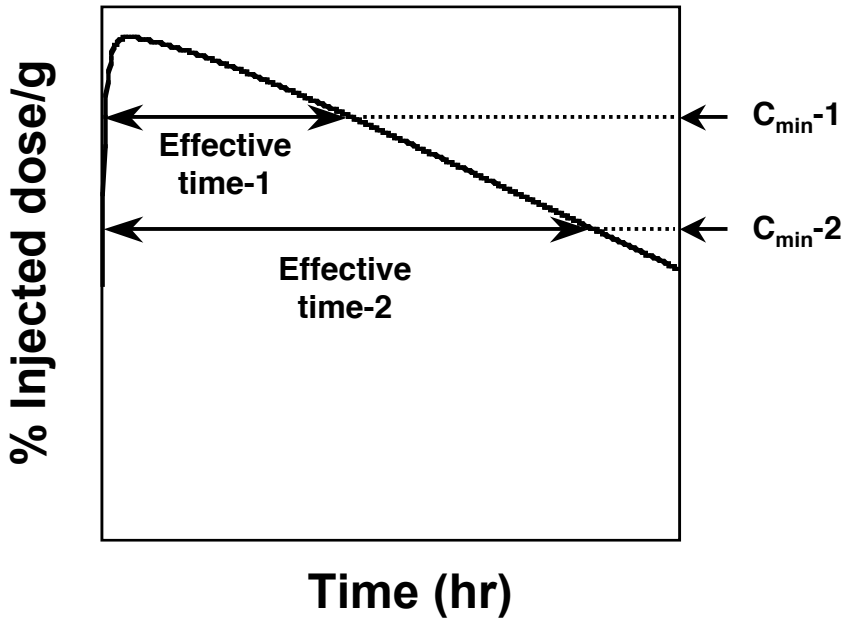
% Injected dose/g
Effective time-1
Effective time-2
C_{min}-1
C_{min}-2
Time (hr)

Scheme 1B

Supplementary Table 1

Relationship between exposure time and IC_{50} *in vitro*

Exposure time (hr)	IC_{50} (nM)	AUC (nM•hr)[a)]
4	**6.7×10^2**	**2.7×10^3**
12	**3.0×10^2**	**3.6×10^3**
24	**0.8×10^2**	**1.9×10^3**
48	**0.7×10^2**	**3.4×10^3**

[a)] AUC = exposure time × IC_{50}

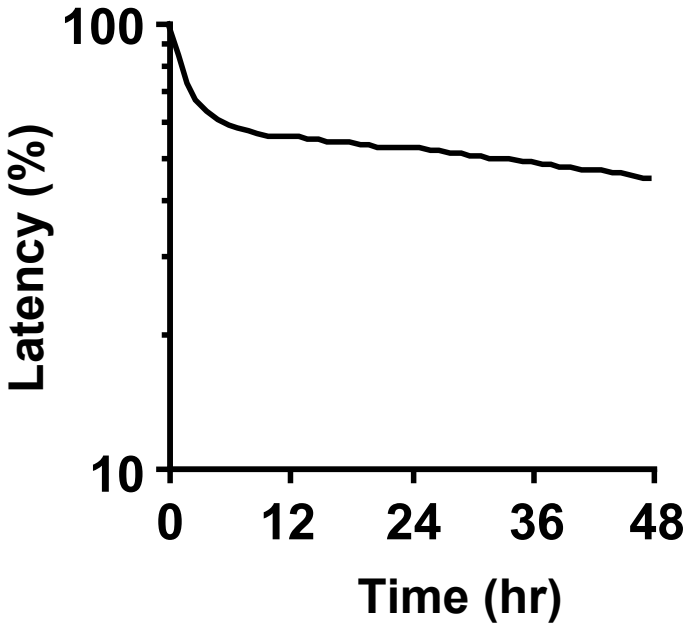

Supplementary Fig. 1
Latency calculated based on the data shown in Fig. 2C.